Birck and NCN Publications   Birck Nanotechnology Center

8-17-2009

Self-supporting nanowire arrays templated in sacrificial branched porous anodic alumina for thermoelectric devices

Kalapi G. Biswas
Purdue University - Main Campus, kgbiswas@purdue.edu

Hatem El Matbouly
Purdue University - Main Campus, helmatbo@purdue.edu

Vijay Rawat
Purdue University - Main Campus

Jeremy L. Schroeder
Birck Nanotechnology Center, Purdue University, jlschroe@purdue.edu

Timothy D. Sands
Purdue University, tsands@purdue.edu

Follow this and additional works at: http://docs.lib.purdue.edu/nanopub

Part of the Nanoscience and Nanotechnology Commons

Self-supporting nanowire arrays templated in sacrificial branched porous anodic alumina for thermoelectric devices

Kalapi G. Biswas,[1,a)] Hatem El Matbouly,[2] Vijay Rawat,[1] Jeremy L. Schroeder,[1] and Timothy D. Sands[1,3]

[1]*School of Materials Engineering and Birck Nanotechnology Center, Purdue University, West Lafayette, Indiana 47907, USA*

[2]*Department of Physics and Birck Nanotechnology Center, Purdue University, West Lafayette, Indiana 47907, USA*

[3]*School of Electrical and Computer Engineering and Birck Nanotechnology Center, Purdue University, West Lafayette, Indiana 47907, USA*

Templated synthesis of thermoelectric nanowires in porous anodic alumina (PAA) have potential for enhanced performance relative to bulk materials. A significant challenge is the template material, which can serve as a thermal shunt. In this work, an approach for creating a branched PAA template is described. The process utilizes localized self-heating to destabilize the planar anodization front, yielding branched and interconnected pores growing at a rate of 300 μm/h. The template is selectively etched after electrodeposition of desired materials, yielding self-supporting nanowire arrays with thicknesses up to about 300 μm, thereby eliminating the thermal shunt through the template. © *2009 American Institute of Physics*. [DOI: 10.1063/1.3207756]

Porous anodic alumina (PAA), also known as anodic aluminum oxide, has been the most widely applied template material for synthesizing nanowire arrays by electrochemical means. Within narrow ranges of anodization conditions—including pH, acid electrolyte, temperature and applied potential—PAA templates can be fabricated with parallel and uniform pores in naturally ordered hexagonal arrays.[1–4] The hexagonal order can be further improved by two-step anodization or by imprinting the aluminum surface to dictate the pore nucleation sites.[5,6] This exquisite self-order and simple processing method exemplifies the most attractive features of nanomanufacturing.

In recognition of the potential of PAA as a matrix for the fabrication of nanowire array thermoelectric materials, several research groups have developed processes for electrodeposition of thermoelectric materials such as Bi_2Te_3, $(Bi,Sb)_2(Te,Se)_3$ alloys, PbTe, and Bi–Sb alloys to fabricate nanowire array composites.[7–11] The original motivation was to improve the properties of these thermoelectric materials by quantum confinement, thereby manipulating the density of states to enhance the power factor,[12] $S^2\sigma$, where S is the Seebeck coefficient in units of V/K and σ is the electrical conductivity in units of Ω^{-1} m^{-1}. The dimensionless figure-of-merit, ZT, for thermoelectric materials is given by $S^2\sigma T/\kappa$, where T is the temperature and κ is the thermal conductivity in units of W/m K. Hence, improving the power factor alone is not sufficient; the lattice thermal conductivity must also be considered. Herein lies the problem with PAA; its thermal conductivity is comparable to the thermal conductivity of the thermoelectric materials of interest.[13–15] Thus, the PAA serves as a thermal shunt that detracts from any gain in the power factor. In fact, gains in the power factor from quantum confinement have not been conclusively demonstrated in materials that yield ZT values approaching or exceeding 1 in bulk form. The required di-

mensions, typically on the order of a few nanometers, and the requisite control of the Fermi energy relative to the van Hove singularities in the density of states, make the goal of quantum enhancement an elusive target. Nevertheless, the nanowire topology does offer advantages of control over crystallographic texture (Bi_2Te_3 nanowires typically adopt a texture that orients the highest ZT directions in the bulk along the wire axis),[16] suppression of lattice thermal conductivity through boundary scattering,[17] and enhanced elastic accommodation of lattice mismatch through relaxation at the free surfaces.[18] These advantages should be realizable at dimensions substantially larger than those required for quantum confinement. Nevertheless, the thermal shunt through the PAA matrix must be mitigated. In previous work, we have shown that it is possible to selectively etch the PAA and replace it with SU-8, a photopolymer with low thermal conductivity.[19] The reduction in thermal conductivity was measured and was found to be in good agreement with a simple composite model.[20] This approach is not easily scalable to thick composites, greater than 100 μm, that are needed to optimize device efficiency with large temperature differences. The use of a polymer matrix also limits the maximum hot-side temperature. A solution to this dilemma would be to design a sacrificial template with interconnected pores that would yield a self-supporting nanowire array upon removal of the template. In the present report, we describe such a process, propose a mechanism for formation of PAA with interconnected pores, and demonstrate the templated synthesis of self-supporting nanowires composed of thermoelectric materials such as Bi_2Te_3.

The conventional method for fabricating PAA templates is by anodic oxidation (anodization) of aluminum foil or films in a slightly acidic electrolytic bath. The simultaneous oxidation and dissolution of Al leads to formation of alumina with self-ordered, vertical pores in a hexagonal arrangement and terminated in a barrier oxide. The pore diameter and interpore spacing depend on the electrochemical conditions, such as the pH and temperature of the electrolytic bath and
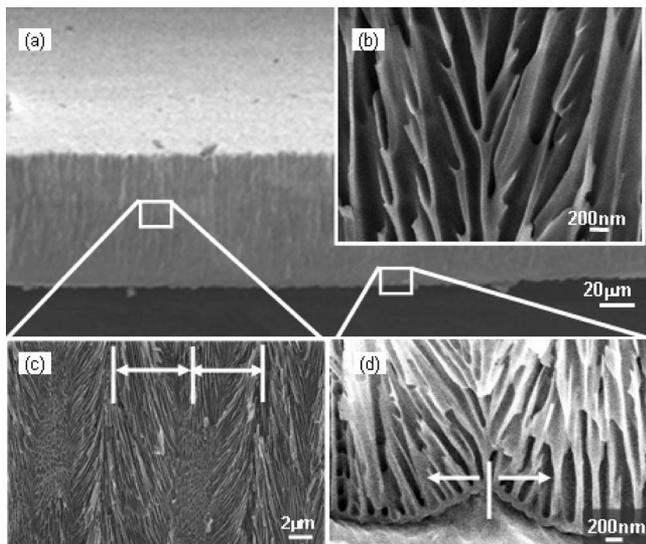
---

a)Electronic mail: kgbiswas@purdue.edu.

FIG. 1. Cross-sectional FESEM images of (a) an interconnected branched porous template showing the total thickness of the template of about 100 μm, (b) a magnified view of a representative region in the B-PAA template displaying the branched network, pore diameter $\sim$200 nm, and pore wall thickness $\sim$20 nm. (c) 3D quasiperiodic network of pores throughout the template and (d) B-PAA/Al interface showing the barrier layer at the bottom of each pore with interpore distance $\sim$500 nm and a larger-scale scalloping of the interface with a period of about $\sim$5 μm.
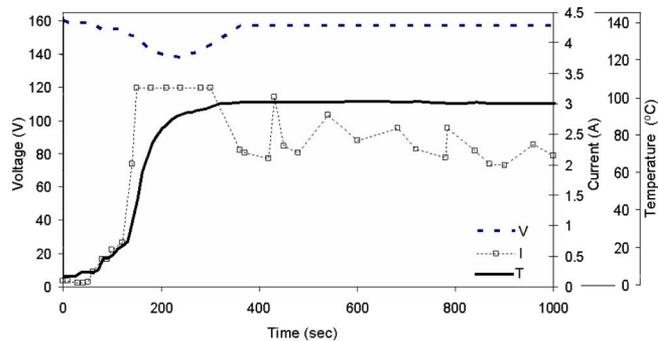

FIG. 2. (Color online) Plot of voltage-current-temperature transient during B-PAA formation. Aluminum is anodized in a 0.4M phosphoric acid electrolyte at a potential of 160 V and a limiting current density of 1.1 A/cm^2 with an initial bath temperature of 4 °C. An initial incubation period is observed during which the current is more typical of MA conditions. This is followed by an increase in bath temperature. The increase in bath temperature increases the ionic conductivity of the barrier oxide. This in turn leads to an increase in current and associated heating. The positive feedback runs the temperature up rapidly until boiling of the electrolyte within the pores interrupts anodization and limits the further rise in bath temperature to 95 °C.

the applied potential or current.[21] The electrolytes generally used for anodization of aluminum are (a) sulfuric acid (H_2SO_4), (b) oxalic acid ($H_2C_2O_4$), and (c) phosphoric acid (H_3PO_4), each with a respective optimum potential for self ordering of pores.[1–4,22–25] The fabrication of PAA with self-ordered pores is called mild anodization (MA), where typical growth rates are 2–5 μm/h. The rapid fabrication of PAA is called hard anodization (HA). HA in sulfuric and oxalic acid electrolytes under approximately three times higher applied potentials enables PAA growth rates that are $\sim$25–35 times faster than MA.[22,26,27] The MA process in phosphoric acid electrolytes is well documented and requires a potential range of 160–195 V to enable vertical pores with a growth rate of about 5 μm/h, current density of $\sim$4 mA cm^{-2}, average pore diameter, D_p, of $\sim$200 nm, and interpore spacing, D_{int}, of $\sim$500 nm. In order to introduce complexity into the template, researchers have demonstrated the fabrication of vertical porous templates with controlled Y branching[28,29] and controlled diameter modulation by altering the anodization potential.[22] However, the porous channels remain vertical before and after the introduction of features at desired thickness intervals, and the junctions where the complex features originate could lead to weak zones in the nanowire arrays. In order to fabricate self-supported nanowire arrays, a template with a three-dimensional (3D) network of branched pores throughout its thickness is needed.

Here we demonstrate the fabrication of 3D branched PAA (B-PAA) templates (Fig. 1) by aggressive anodization of aluminum. Aluminum (99.9995% purity, 1 mm thick foil; PVD Materials Corp.) was cleaned with acetone and methanol and then electropolished in a solution composed of 5 vol % sulfuric acid, 95 vol % phosphoric acid, and 20 g/l chromic oxide using a potential of 20 V for 20 s. After electropolishing both sides, the aluminum foil was anodized in a 0.4M phosphoric acid using a potential of 160 V and a stabilized current density of 1.1 A/cm^2. The initial electrolytic

bath temperature was maintained at 4 °C. During anodization under these conditions, the bath temperature increased rapidly from 4 to $\sim$95 °C. The electrolyte was continuously replenished to maintain the meniscus level and a constant sample area that was being anodized. The voltage-current-temperature transient during B-PAA formation (Fig. 2) indicates an incubation period (0–30 s) where the potential is 160 V, current is 0.05 A (current density 15 mA/cm^2) and temperature is 4 °C. The initial pore formation occurs during this incubation period. As the bath temperature increases, the ionic conductivity of the barrier oxide increases. This in turn leads to an increase in current and associated heating. The positive feedback runs the temperature up rapidly until boiling of the electrolyte within the pores interrupts anodization and limits the further rise in bath temperature. At the steady state temperature, an equilibrium barrier thickness is established by branching of smaller pores from self-selected primary pores that are separated laterally by $\sim$5 μm. Because the secondary pores nucleate at the base of the primary pore, the secondary pores fan out, yielding a scalloped growth front with an approximate spacing between protrusions of about 5 μm, and a single dominant primary pore at the center of each protrusion. The resulting microstructure consists of "supercells" that terminate in the scalloped protrusion. The secondary pores at the boundaries of each supercell intersect with the secondary pores from the adjacent protrusion, leading to an interconnected pore network. This structure is retained through the anodization process, with only minor coarsening of the supercells. A detailed study of the B-PAA formation process under a range of conditions will be reported elsewhere. After the anodization step, the nonanodized aluminum at the bottom of the B-PAA template was removed by floating the sample in a solution composed of 10 wt % mercury dichloride for 4 h. The barrier oxide at the bottom of the pores in the alumina film was removed by immersing the sample in a 2M KOH solution at 60 °C, followed by mechanical polishing on both sides.

Figure 1(a) presents a cross-sectional field emission scanning electron microscope (FESEM) image of a $\sim$100 μm thick interconnected B-PAA template. A high
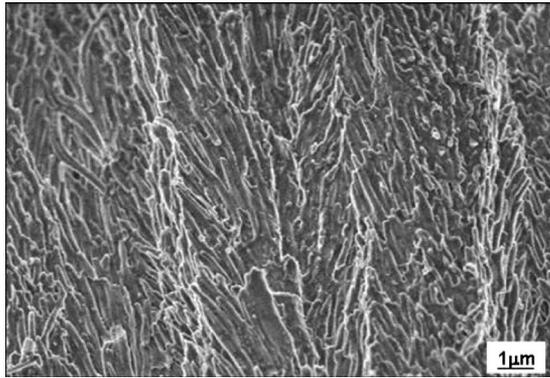
FIG. 3. Cross-sectional FESEM image of fractured self-supporting Bi_2Te_3 nanowire array after selective etching of the B-PAA in $3M$ KOH solution, displaying the conformity of the nanowires to the shape of the branched porous network and mechanical integrity of the fractured surface.

magnification cross-sectional image of B-PAA [Fig. 1(b)] confirms the branched network of pores with average pore diameters of approximately 200 nm and pore wall thickness of about 20 nm. Figure 1(c) shows a representative cross-sectional image corresponding to the middle of a B-PAA template, which reveals the 3D network of primary and secondary pores that is quasiperiodic throughout the template. A cross-sectional image at the bottom of the B-PAA template— the metal/oxide interface [Fig. 1(d)] shows the barrier layer at the bottom of each pore, and a larger scale "scalloping" of the interface with a spatial periodicity of ~ 5 μm. The spacing between adjacent supercells is about an order of magnitude larger than the initial interpore spacing.

The formation of B-PAA is much faster than the formation of conventional PAA by MA or HA in sulfuric or oxalic acid. The growth rate in B-PAA formation is ~ 300 μm/h, about 60 times faster than PAA fabricated by MA. The current density during B-PAA formation (1.1 A/cm^2) is three orders of magnitude higher than the current density during PAA formation under MA conditions (4 mA/cm^2).

To demonstrate the utility of these B-PAA templates in fabricating self-supporting nanowires of thermoelectric materials, nominally 400 μm thick B-PAA templates were mechanically polished on both sides and etched in phosphoric acid to clear debris from the pore openings. Platinum was deposited using e-beam evaporation on one side (i.e., the Al-facing side) of the template to serve as a back electrode for electrodeposition. Bi_2Te_3, $(Bi,Sb)_2Te_3$, and PbTe were electrodeposited under conditions similar to those used for nanowire growth in PAA templates. The electrolyte for Bi_2Te_3 nanowires consisted of $0.035M$ $Bi(NO_3)_3 \cdot 5H_2O$ and $0.05M$ $HTeO_2^+$ in $1M$ nitric acid, and a $pH=1$ was maintained throughout the process. The nanowires were electrodeposited using 3 s pulses of current density 5 mA/cm^2 followed by a standby period of 3 s. The $(Bi,Sb)_2Te_3$ and PbTe nanowires were electrodeposited under potentiostatic conditions of -100 and -800 mV, respectively. The electrolyte for $(Bi,Sb)_2Te_3$ consisted of $1 \times 10^{-2}M$ $HTeO_2^+$, $0.84M$ tartaric acid, $2.4 \times 10^{-3}M$ Bi, $5 \times 10^{-3}M$ SbO^+ in $1M$ HNO_3 and that for PbTe consisted of $0.01M$ $HTeO_2^+$, $0.05M$ Pb_2^+ in $1M$ HNO_3. A fracture cross section of a Bi_2Te_3 nanowire array after selective etching of the B-PAA in $3M$ KOH solution (24 h) is shown in Fig. 3. Similar results (not shown)

have been achieved in the $(Bi,Sb)_2Te_3$ and PbTe materials systems.

In conclusion, the process demonstrated here for fabricating self-supporting interconnected nanowire arrays effectively eliminates the thermal shunt from the template, thereby allowing for the full benefit of the nanowire topology in nanostructured thermoelectric elements. The high rate of B-PAA formation allows for sacrificial templates that are thicker than 100 μm, thereby mitigating the deleterious effect of electrical contact resistance on element performance. Although the present work has been presented in the context of thermoelectric devices, the same process can be employed to generate dense, self-supporting nanowire arrays for nanostructured batteries, gas and liquid-phase sensors, optical coatings, and photovoltaic devices.

[1] H. Masuda and K. Fukuda, Science **268**, 1466 (1995).
[2] K. Nielsch, J. Choi, K. Schwirn, R. B. Wehrspohn, and U. Gösele, Nano Lett. **2**, 677 (2002).
[3] H. Masuda, F. Hasegwa, and S. Ono, J. Electrochem. Soc. **144**, L127 (1997).
[4] A. P. Li, F. Muller, A. Birner, K. Nielsch, and U. Gosele, J. Appl. Phys. **84**, 6023 (1998).
[5] H. Masuda, H. Yamada, M. Satoh, H. Asoh, M. Nakao, and T. Tamamura, Appl. Phys. Lett. **71**, 2770 (1997).
[6] J. Choi, K. Nielsch, M. Reiche, R. B. Wehrspohn, and U. Gosele, J. Vac. Sci. Technol. B **21**, 763 (2003).
[7] M. S. Sander, A. L. Prieto, R. Gronsky, T. Sands, and A. M. Stacy, Adv. Mater. **14**, 665 (2002).
[8] C. G. Jin, X. Q. Xiang, C. Jia, W. F. Liu, W. L. Cai, L. Z. Yao, and X. G. Li, J. Phys. Chem. B **108**, 1844 (2004).
[9] M. Sima, I. Enculescu, and E. Vasile, Rom. Rep. Phys. **58**, 183 (2006).
[10] F. H. Xue, G. T. Fei, B. Wu, P. Cui, and L. D. Zhang, J. Am. Chem. Soc. **127**, 15348 (2005).
[11] B. Yoo, F. Xiao, K. N. Bozhilov, J. Herman, M. A. Ryan, and N. V. Myung, Adv. Mater. **19**, 296 (2007).
[12] L. D. Hicks and M. S. Dresselhaus, Phys. Rev. B **47**, 16631 (1993).
[13] D.-A. Borca-Tasciuc, G. Chen, A. Prieto, M. S. Martín-González, A. Stacy, T. Sands, M. A. Ryan, and J. P. Fleurial, Appl. Phys. Lett. **85**, 6001 (2004).
[14] J. H. Zhou, C. G. Jin, J. H. Seol, X. G. Li, and L. Shi, Appl. Phys. Lett. **87**, 133109 (2005).
[15] D. A. Borca-Tasciuc and G. Chen, J. Appl. Phys. **97**, 084303 (2005).
[16] I. Trahey, C. R. Becker, and A. Stacy, Nano Lett. **7**, 2535 (2007).
[17] A. Hochbaum, R. Chen, R. D. Delgado, W. Liang, E. C. Garnett, M. Najarian, A. Majumdar, and P. D. Yang, Nature (London) **451**, 163 (2008).
[18] E. Ertekin, P. A. Greaney, D. C. Chrzan, and T. D. Sands, J. Appl. Phys. **97**, 114325 (2005).
[19] K. G. Biswas, Proceedings of 2nd Energy Nanotechnology International Conference, 2007 (unpublished).
[20] K. G. Biswas, B. A. Cola, X. Xu, and T. D. Sands, Appl. Phys. Lett. **94**, 223116 (2009).
[21] G. E. Thompson and G. C. Wood, in *Treatise on Materials Science and Technology*, edited by C. Scully (Academic, New York, 1983).
[22] W. Lee, R. Ji, U. Gosele, and K. Nielsch, Nature Mater. **5**, 741 (2006).
[23] H. Masuda, K. Yada, and A. Osaka, Jpn. J. Appl. Phys., Part 2 **37**, L1340 (1998).
[24] F. Li, L. Zhang, and R. Metzger, Chem. Mater. **10**, 2470 (1998).
[25] O. Jessensky, F. Muller, and U. Gosele, Appl. Phys. Lett. **72**, 1173 (1998).
[26] S. Z. Chu, K. Wada, S. Inoue, M. Isogai, and A. Yasumori, Adv. Mater. **17**, 2115 (2005).
[27] S. Z. Chu, K. Wada, S. Inoue, M. Isogai, Y. Katsuta, and A. Yasumori, J. Electrochem. Soc. **153**, B384 (2006).
[28] J. Choi, G. Sauer, K. Nielsch, R. B. Wehrspohn, and U. Gosele, Chem. Mater. **15**, 776 (2003).
[29] T. Gao, G. Meng, J. Zhang, S. Sun, and L. Zhang, Appl. Phys. A: Mater. Sci. Process. **74**, 403 (2002).